Cis – Trans Photoisomerization of Fluorescent-Protein Chromophores

ARTICLE *in* THE JOURNAL OF PHYSICAL CHEMISTRY B · SEPTEMBER 2008

Impact Factor: 3.3 · DOI: 10.1021/jp802419h · Source: PubMed

Cis−*Trans* Photoisomerization of Fluorescent-Protein Chromophores

Valerio Voliani,*,† Ranieri Bizzarri,†,‡ Riccardo Nifosì,†,‡ Stefania Abbruzzetti,§ Elena Grandi,§ Cristiano Viappiani,§ and Fabio Beltram†,‡

Scuola Normale Superiore, Italian Institute of Technology, Piazza dei Cavalieri 7, I-56126 Pisa, Italy, NEST, Scuola Normale Superiore and CNR-INFM, via della Faggiola 19, I-56126 Pisa, Italy, and NEST CNR-INFM, Dipartimento di Fisica, Università di Parma, viale G. P. Usberti 7A, I-43100 Parma, Italy

Received: March 19, 2008; Revised Manuscript Received: June 5, 2008

Photochromic variants of fluorescent proteins are opening the way to a number of opportunities for high-sensitivity regioselective studies in the cellular environment and may even lead to applications in information and communication technology. Yet, the detailed photophysical processes at the basis of photoswitching have not been fully clarified. In this paper, we used synthetic FP chromophores to clarify the photophysical processes associated with the photochromic behavior. In particular, we investigated the spectral modification of synthetic chromophore analogues of wild-type green fluorescent protein (GFP), Y66F GFP (BFPF), and Y66W GFP (CFP) upon irradiation in solutions of different polarities. We found that the *cis*−*trans* photoisomerization mechanism can be induced in all the chromophores. The structural assignments were carried out both by NMR measurements and DFT calculations. Remarkably, we determined for the first time the spectra of neutral *trans* isomers in different solvents. Finally, we calculated the photoconversion quantum yields by absorption measurements under continuous illumination at different times and by a nanosecond laser-flash photolysis method. Our results indicate that *cis*−*trans* photoisomerization is a general mechanism of FP chromophores whose efficiency is modulated by the detailed mutant-specific protein environment.

Introduction

Fluorescent proteins (FPs) are arguably the most important fluorescent probes in molecular biology.[1,2] This largely stems from the fact that their primary sequence can provide all the information needed for fluorescence expression. As a consequence fluorescent fusion constructs consisting of a given protein of interest and an FP can be rather straightforwardly expressed in living cells.[1] The green fluorescent protein (GFP) from jellyfish *Aquorea victoria* was the first such protein to be discovered and cloned in eukariotes. GFP is the ancestor of the most widespread FP family for *in vivo* detection.[2]

The chromophore of GFP is a *p*-hydroxybenzylidene imidazolinone that is generated by the subsequential cyclyzation/oxidation/dehydration of the Ser^{65}-Tyr^{66}-Gly^{67} motif, on the aftermath of the primary sequence folding into a β-barrel tertiary structure.[3] Successful engineering of both absorption and emission spectra of GFPs was achieved by substituting selected aminoacids in the primary sequence.[4] Blue-shifted variants of parent GFP were obtained by replacing Tyr^{66} with triptophan (cyan fluorescent protein, CFP), histidine (blue fluorescent protein, BFP), or phenylalanine (Y66F GFP, hereafter denoted as BFPF).[5] The reduced electron conjugation in the chromophore when an indolyl, imidazolyl or phenyl ring replaces the phenol of GFP accounts for the blue-shifted fluorescence of these mutants. Despite lower quantum yield and photostability with respect to GFP, these mutants found widespread use in cellular multitracking studies,[8] colocalization analyses,[9] and as donors in fluorescence resonance energy transfer (FRET) *in vivo* measurements with green[10] or yellow FPs as acceptors.[6]

Recently, the use of photoswitchable proteins for *in vivo* studies has attracted wide interest.[12–14] Irreversibly photoswitchable variants from dark to bright states[7] or from one color to another[8] expanded noticeably the range of applications of conventional FPs.[17–19] In 2003 we suggested that the dark state of photoswitching GFP mutants, including one developed by us,[9] carried a *trans* chromophore configuration (in contrast to the normal *cis* configuration) achieved through *cis*−*trans* photoisomerization around the exocyclic double bond.[10] Our argument was based on theoretical calculations and indirect spectral evidence, and referred also to photophysical studies carried out on models of the GFP chromophore.[22–26] Such a photoinduced *cis*−*trans* isomerization was recently demonstrated by X-ray analysis for a FP variant from *Anemonia Sulcata*,[11] for a mutant derived from *Clavularia*,[12] and for the popular Dronpa variant from *Pectidinaee*.[13] In spite of a poor homology in primary sequence, these proteins display β-barrel tertiary structures and highly conjugated imidazolinone chromophores resembling those of GFP. *Cis*−*trans* photoisomerization is presumably a general feature of this large class of chromophores. Indeed, photoinduced *cis*−*trans* isomerization was verified experimentally at least for HBDI, a synthetic analogue of the wtGFP chromophore.[10] The optical and photochromic properties of the *trans* state, however, were not reported.

It is worth noting that the FP photochromism is a complex molecular process for which a loss of structural rigidity of the chromophore in the protein barrel is the determining factor.[12,14,15] Additionally, for some proteins a proton transfer step seems to be related to the structural change associated with photochromism. The photophysical properties of the *cis*−*trans* isomerization must be interpreted in such a perspective. Indeed, the most relevant structural feature to allow the *cis*−*trans* isomerization is the possibility of a concerted torsion around

* To whom correspondence should be addressed. E-mail: v.voliani@sns.it.
† Scuola Normale Superiore, Italian Institute of Technology.
‡ NEST, Scuola Normale Superiore and CNR-INFM.
§ NEST CNR-INFM, Dipartimento di Fisica, Università di Parma.

10.1021/jp802419h CCC: $40.75
Published on Web 07/31/2008

SCHEME 1: Chemical Synthesis (i−ii) and Reversible *Cis*−*Trans* Photoisomerization of Chromophores (iii−iv)[a]

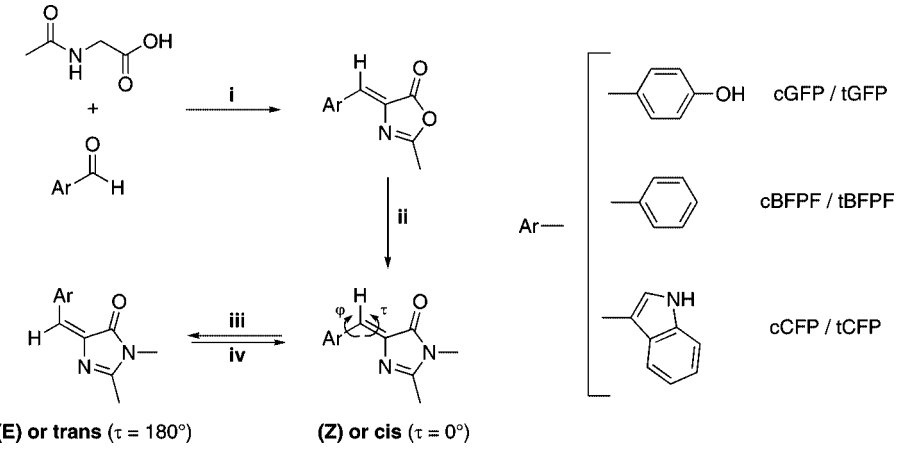

[a] Key: (**i**) CH_3COONa, $(CH_3COO)_2$, 110−130 °C; (**ii**) $CH_3NH_{2(aq)}$, ethanol, Na_2CO_3, 120−130 °C; (**iii**) hν; (**iv**) hν and/or Δ. The stereochemically-relevant dihedral angles φ and τ are shown: *cis* and *trans* configurations correspond to $\tau = 0°$ and $\tau = 180°$, respectively.

the bonds connecting the two rings, which results in a space-saving isomerization mechanism termed *hula-twist*.[16] We believe that detailed understanding of the FP photochromism requires a comparison between the photoisomerization efficiency of the chromophore alone and when embedded in the protein barrel.

On account of our long-standing interest in the photophysical properties of FPs,[4,9,10,17] we set off to investigate how the chromophore structure influences the *cis*−*trans* photoisomerization and the optical differences between the two states. In this paper we report on our studies regarding the photoisomerization of synthetic analogues of the GFP, CFP, and BFPF chromophores in solutions of different polarities. We shall show by optical and NMR measurements and by computer modeling, that the same photoinduced, reversible *cis*−*trans* mechanism is shared by all these chromophores. We shall argue that this result supports the idea that reversible *cis*−*trans* isomerization is a general photoprocess that does or does not take place in a given folded mutant on account of the detailed local chromophore environment. In addition, we shall report for the first time the absorption spectra of the *trans* chromophores and quantify the efficiency of the photoisomerization process. These data will be compared with the reported photoconversion efficiencies of some FPs, in view of estimating the role of protein matrix rigidity on the emergence of the photochromic protein properties.

Materials and Methods

Chromophore Synthesis. The chromophores were synthesized according to the established procedure, involving the preliminary synthesis of azalactone compounds followed by their aminolysis with methylamine.[18] The details of this procedure are reported as Supporting Information.

Absorption Spectroscopy. Ultraviolet−visible (UV−vis) spectra were measured on a Jasco 550 spectrophotometer (Jasco, Tokyo, Japan) supplied with a Jasco ETC-505T thermostat.

NMR Spectrometry. NMR spectra were collected by Varian Unity 300 spectrometer (Varian, Palo Alto, CA, USA) at room temperature on 5−10% solutions in DMSO-d_6, Dioxane-d_8, or $CDCl_3$. ^{1}H NMR spectra were collected at 300 MHz with the follow experimental conditions: 32768 points, 3 kHz of spectral width, 30° impulse, 2 s acquisition time, and 1024 transients. ^{13}C NMR spectra were collected at 75 MHz with the following experimental conditions: 65536 points, 15 kHz of spectral width, 70° impulse, 0.8 s acquisition time, and $(1-2) \times 10^5$ transients.

Photoconversion Experiments. Solutions of chromophore or protein in water at pH 6.5−7 or organic solvents were placed in 1500 μL quartz cells with a 1 cm path length for absorption spectroscopy experiments; solutions with concentration 1 to 10 mM were placed into 700 μL quartz cells with a 0.5 cm path length for NMR spectrometry experiments. Photoconversion was obtained by irradiating at 360, 406, or 458 nm by using either an Ar−Kr laser (Beamlok 2060, Spectra Physics, Mountain View, CA).Temperature was controlled by a Peltier thermostat (Varian, Palo Alto, CA) and continuous stirring was ensured.

Nanosecond Laser Flash Photolysis. Laser flash photolysis experiments were performed with a previously described setup.[19,20] Photoexcitation was achieved by the third harmonic (355 nm) of a nanosecond Nd:YAG laser, and detection of the absorbance change was performed with the cw output of a Xe arc lamp and a Si photodiode as a detector (see Supporting Information for further details).

Theoretical Calculations. We evaluated the excitation energies using the time-dependent extension of DFT in the linear perturbation theory,[17] with B3LYP exchange and correlation functional[21] and 6-31+G* basis set, on structures optimized with B3LYP/6-31G*. We included implicit solvent effects through the polarizable continuum method (PCM).[10] The performance of these techniques for fluorescent protein chromophores were analyzed elsewhere.[17] The ^{13}C NMR chemical shifts were calculated by the GIAO method[22] (B3LYP/6-311G**), on structures optimized at the same level of theory. Since the two pairs of opposite carbons on the benzene ring are equivalent on the time scale of the NMR experiment, the average chemical-shift value was taken for comparison with experiment. Gaussian 03[23] was used for the calculations.

Results

Synthesis of GFP Chromophores. The synthesis of model chromophores was accomplished by means of an established synthetic procedure involving two steps (Scheme 1, reactions **i**−**ii**). Note that, unless sterically hindered reactants are used in the first step, this procedure is known to yield (*Z*)-isomers.[24,25] The higher thermodynamic stability of the (*Z*)-isomers of our chromophores was indeed predicted by theoretical calculations (see below). For clarity of discussion, we will refer to the (*Z*)- and (*E*)-isomers as *cis* and *trans*, respectively, in agreement with the practical nomenclature commonly adopted for the chromophores of FPs. The prefixes c and t will be added to the

TABLE 1: Calculated Stereochemical Free-Energy G(φ,τ) and Dipole Moments μ and Measured Photoisomerization Quantum Yields Φ

chromophore	φ (deg)	τ (deg)	μ (D)	G(φ,τ)[a] met[c] (kcal/mol)	G(φ,τ)[a] wat[d] (kcal/mol)	G(φ,τ)[a] gp[b] (kcal/mol)	Φ[f]
cGFP	0.0 (180°)	0.0	3.65	0[e]	0	0	0.21 ± 0.01[g]
							0.21 ± 0.05[h]
tGFP	0.0 (180°)	180	2.00	2.43	2.47	2.41	0.18 ± 0.02[g]
cBFPF	0.2 (179.8°)	0.0	3.43	0	0	0	0.10 ± 0.0 + 2[g]
							0.08 ± 0.05[h]
tBFPF	0.6 (179.4°)	180	2.21	2.67	2.72	2.76	~1[f]
c1CFP	0.1	0.0	6.57	0	nc[e]	0	0.2 ± 0.1[g]
							0.24 ± 0.13[h]
c2CFP	179.9	0.0	3.46	1.04	nc[e]	1.44	nc[e]
t1CFP	0.8	179.9	2.60	0.99	nc[e]	0.573	0.9 ± 0.3[g]
t2CFP	177.8	179.4	4.22	6.49	nc[e]	7.51	nc[e]

[a] $G(0,0)$ was set to 0 as reference for each chromophore. [b] gp: gas phase. [c] met: methanol. [d] wat: water. [e] nc: not calculated. [f] Photoisomerization quantum yield. [g] from continuous irradiation experiments. [h] From flash photolysis experiments.

chromophore name to identify its stereoisomeric form (e.g., cGFP: *cis*-GFP chromophore). Furthemore, we shall adopt the protein data bank (PDB) nomenclature of FPs to denote specific atoms in the chromophores.[26]

Thermodynamic Stability As a Function of Chromophore Stereochemistry. Given the planarity of the imidazolinone and aromatic rings and the symmetry of the methyl groups, the stereochemical configuration of the chromophores is mainly defined by the φ and τ dihedral angles, which refer to the torsion of the exocyclic C−C or the C═C bonds respectively (Scheme 1). *Cis* and *trans* isomers correspond to $\tau \approx 0°$ and $\tau \approx 180°$, respectively. To assess the relative thermodynamic stability of distinguishable stereochemical configurations, we carried out DFT-B3LYP energy calculations on each chromophore by assuming either gas phase as medium or an implicit solvent of high polarity (methanol or water). Note that solvation free-energy terms (PCM method) are always taken into account when the implicit solvent is added and the vibrational entropy was found to be nearly unaffected by stereochemical changes (~0.1 kcal/mol). Thus, the obtained energy values can be identified with stereochemical free-energies and are denoted by G(φ,τ) (Table 1).

cGFP, tGFP, cBFPF, and tBFPF are all characterized by a symmetrical phenol /phenyl ring, leading to a 2-fold symmetry for rotation around φ. We found that in all four structures the minimum-energy configuration is nearly planar—i.e. ($\varphi \approx 0°$, $\tau \approx 0°$) for *cis* isomers and ($\varphi \approx 0°$, $\tau \approx 180°$) for *trans* isomers—providing extended electronic conjugation while avoiding steric hindrance. Note that the finite tolerance of the optimization procedure is likely at basis of the slight, i.e. <2°, deviations from the perfect all-planar configuration ($\varphi = 0°$, $\tau = 0°$) found in these cases.

The calculated values indicate that cGFP → tGFP isomerization is associated with $\Delta G_i = G_{trans} - G_{cis} = 2.41-2.47$ kcal/mol (Table 1), in good agreement with data reported previously ($\Delta G_i = 2.10$ kcal/mol).[27] cBFPF→tBFPF isomerization is associated with an even larger free-energy change (Table 1). Hence, about 98−99% of molecules of these chromophores must be in the *cis* state at room temperature. Pleasantly, the ^{1}H NMR spectra of cGFP and cBFPF showed resonances attributable to a single stereoisomer (data not show).

The asymmetric indolyl ring of CFP chromophore disrupts the 2-fold symmetry for rotation around φ. Accordingly, the theoretical calculation showed that cCFP and tCFP are both characterized by two energy minima, each one corresponding to a nearly all-planar configuration, which were denoted as c1CFP/c2CFP and t1CFP/t2CFP, respectively (Scheme 2). We found that t1CFP is more stable than c2CFP in all media (Table 1). On the other hand, t2CFP has a very high relative G(φ,τ), likely owing to the unfavorable steric relationship between the indolyl and the imidazolinone rings (Scheme 2), which leads to the highest stereochemical distorsions from the all-planar configuration. From the free-energy values in methanol we calculated that at room temperature 73.5%, 12.5%, 14%, and $<10^{-3}$ % of the chromophore are in the c1CFP, c2CFP, t1CFP, and t2CFP configurations, respectively. The ^{1}H NMR spectrum of cCFP in deuterated methanol at room temperature strongly substantiated these results, as it evidenced that around 12% of the chromophore is in a different stereoisomeric form, lately identified with the *trans* form (see below).

SCHEME 2: Stereochemical Configurations of CFP Chromophore Corresponding to the Energy Minima Calculated by the DFT-B3LYP Method

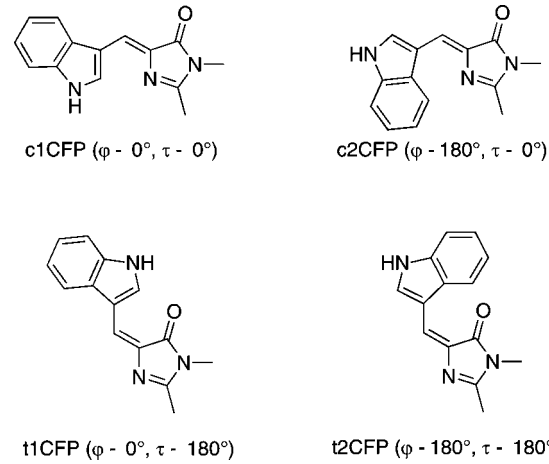

Photoconversion of Chromophores. The absorption spectra of the neutral *cis* chromophores are characterized by two main bands: one, more intense, peaked in the 340−400 nm range (low-energy band), and one, less intense, peaked between 260 and 300 nm (high energy band) (Figure 1a, black trace). On the basis of the TD-DFT B3LYP methods, we assigned the two bands to the HOMO->LUMO and to the HOMO-3->LUMO transitions, respectively. Owing to the ionization of the phenolic group and the formation of a highly conjugated anionic imidazolinone,[28] the low-energy band of cGFP in alkaline water (pH 12) is red-shifted of about 56 nm (not shown).

In the typical photoconversion experiment, a *cis* chromophore was irradiated close to the low-energy band maximum for times ranging from few seconds to 10 min by means of 1−5 mW continuous laser light. The irradiation experiments were carried out in solvents of different characteristics, namely methanol

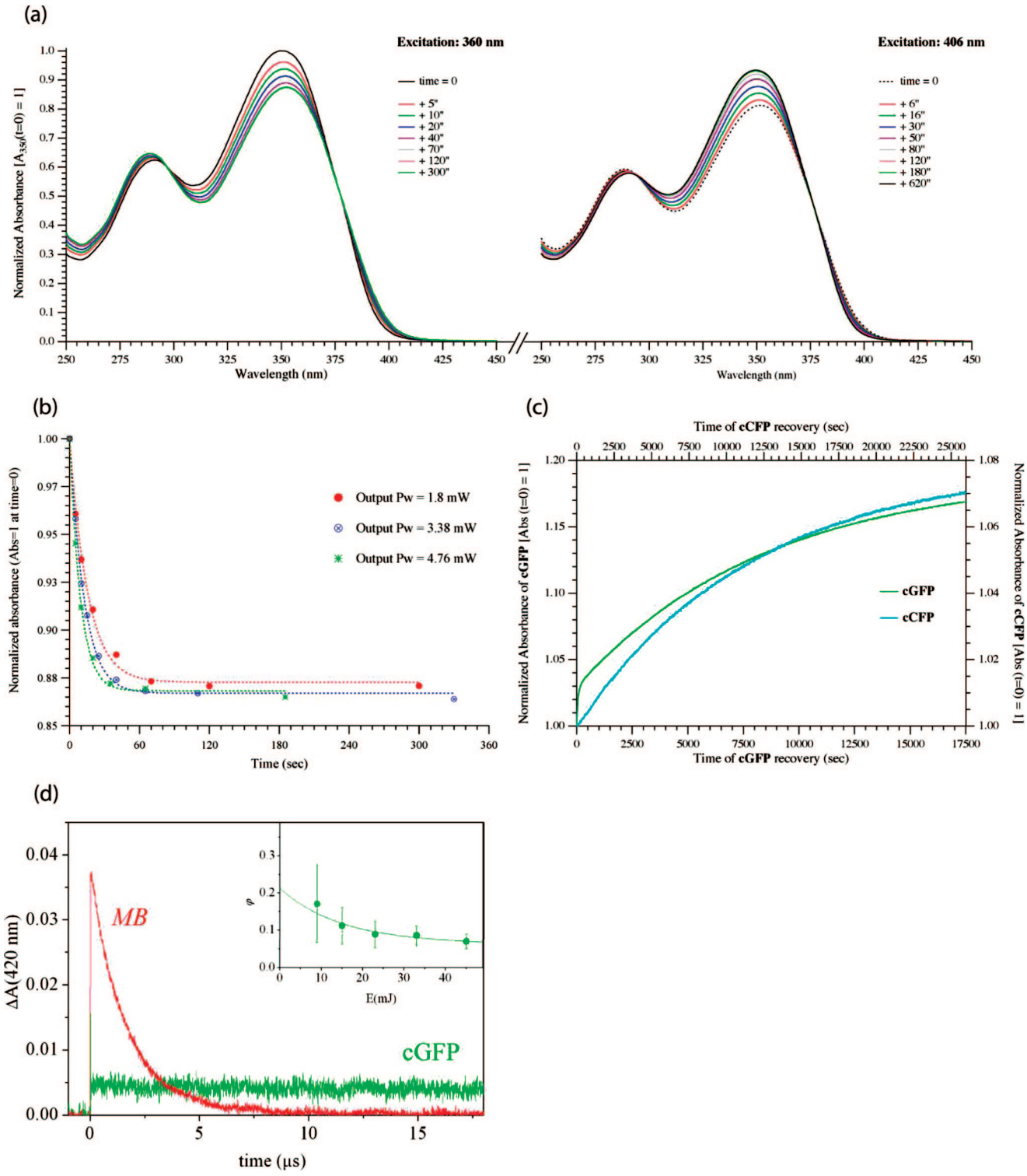

Figure 1. Photochromic characteristics of chromophores. They are exemplified by the optical behavior of cBFPF upon irradiation. (a, left panel) Continuous irradiation at 360 nm leads to the time-dependent decrease and red-shift of the absorption spectrum due to the formation of a photoproduct (identified with tBFPF by NMR, see text); (a, right panel) constant irradiation of photoconverted cBFPF at 406 nm, leads to the reversion of the absorption spectrum. b) The photoconversion rate of cBFPF at 360 nm is dependent on irradiation light power, but the same photostationary state is always achieved; photoconversion curves are fitted to eq S6 (Supporting Information) to yield the photoisomerization quantum yields (see text). (c) Spontaneous recovery to the native state of the photoproducts of cGFP (green line, 360 nm-absorbance) and cCFP (cyan line, 406 nm-absorbance) in methanol at 20 °C. (d) Single high-energy pulse irradiation at 355 nm of cGFP in methanol (OD = 0.6) leads to a fast and irreversible absorption change (<5 ns) detected at 420 nm (green line); methylene blue in water (OD = 0.67) irradiated at the same wavelength shows a fast conversion to triplet state followed by slower (a few microseconds) decay to the ground singlet state because of quenching by molecular oxygen (red line). (inset) By using methylene blue as an actinometer (see text), the comparative method[32] yields φ_c as a function of laser-pulse energy: extrapolation to zero energy gives the actual φ_c value.

(protic solvent, $\epsilon_r = 33$), acetonitrile (aprotic solvent, $\epsilon_r = 36.6$), dioxane (aprotic solvent, $\epsilon_r = 2.2$), and, for cGFP, also in neutral or alkaline water (protic solvent, $\epsilon_r = 80.1$). Indeed, the internal environment of the proteins is typically different from pure water

and in some cases can be strongly hydrophobic. We selected these solvents to explore a large interval of polarity, as expressed by their dielectric constants, and the capability to establish or not hydrogen bonds with the chromophore molecules. Note that methanol and acetonitrile have approximately the same polarity, although only the former solvent is able to partecipate to H-bonding with the chromophores.

In all cases, steady-state photoexcitation led to the decrease in intensity and red-shift of the low-energy band (Figure 1a, left panel); conversely, the high energy band was enhanced upon irradiation. Remarkably, the presence of two sharp isosbestic points indicated the direct conversion of the native chromophore in a photoproduct with different spectral properties. As expected, the rate of photoconversion increased with the excitation power (Figure 1b). For each chromophore the same constant spectrum was asymptotically reached regardless of the irradiation power, thus suggesting that a common photostationary state, characterized by equal forward and reverse light-induced photoconversion rates, had been achieved (Figure 1b).

An optical state close to the native one was restored upon irradiation of the photoproduct at longer wavelengths (>40 nm from the maximum of the *cis* chromophore, Figure 1a, right panel). Again, the process rate was found to increase with the excitation source power. Hence, we concluded that these compounds displayed reversible photochromism. The nature of the solvent did not change the observed photochromic pattern (data not shown).

Interestingly, the photoproducts of cGFP and cCFP were found to decay back to the native state when kept at room temperature and in the dark (Figure 1c). This process was found to be much faster (minutes/few hours) in protic solvents than in aprotic ones (some hours/days). In contrast, the photoproduct of cBFPF remained stable for weeks in all solvents. In methanol at 20 °C, the photoproduct of cGFP relaxed back thermally to their native states following a nonmonoexponential kinetics, whereas the data of cCFP should be fitted to a monoexponential law, with $\tau_2 = 195$ min. To unveil any pH effect on the spontaneous recovery, we also separately addressed the neutral and anionic forms of cGFP. In both cases we found nonmonoexponential decay kinetics much faster than recorded in methanol (not shown), but pH did not change significantly the average time-constant when data were fitted to a biexponential law (pH 6.1, $\langle\tau\rangle = 8.1$ min; pH 10.2, $\langle\tau\rangle = 8.3$ min).

^{1}H NMR Analysis of the Photoproduct. We compared the ^{1}H NMR resonances of each photoproduct with those of the parent *cis* isomer, in view of assessing the structural changes associated with the photoconversion. Deuterated dioxane was chosen as solvent owing to the slow thermal recovery of the photoproducts of cGFP and cCFP to the native state.

The most interesting resonance pattern changes were detected in the 6.5−9.0 ppm aromatic region. The photoproduct of cGFP was found to display a downfield shift of the HD1, HD2, and HB2 proton resonances, whereas HE1 and HE2 were only slightly affected (Figure 2a). Remarkably, similar spectral changes were described for irradiated cGFP in deuterium oxide,[27] deuterated DMSO,[29] and deuterated methanol.[29] Consistently with these authors, we can identify the photoproduct with the *trans* isomer tGFP upon analogy with the ^{1}H NMR spectra of structurally related azlactone moieties.[30] Similar resonance shifts were observed for the photoproducts of cBFPF and cCFP (Figure 2a), which were accordingly identified with tBFPF and tCFP. From peak integration, we calculated that tGFP, tBFPF, and tCFP represent the 57%, 71%, and 76% of the moles in the photoirradiated mixtures, respectively.

^{13}C NMR Structural Identification of the Photoproduct of cBFPF. To further confirm the identification of the photoproducts with the *trans* isomers, we carried out a thorough ^{13}C NMR analysis on cBFPF before and after irradiation. This chromophore was selected for its simpler structure and because it did not show thermal recovery to the native state. Deuterated dioxane was chosen as solvent owing to its aprotic and apolar nature that prevents large modifications of the NMR pattern provoked by strong solvent−solute interactions.

The fully decoupled ^{13}C NMR spectrum of the photoproduct resembled closely that of cBFPF, although it was on average shifted 6−8 ppm downfield. Under the assumption of *cis-trans* isomerization, we carried out GIAO/DFT calculations of the chemical shifts of both isomers and we compared them with those retrieved experimentally. The ^{13}C NMR pattern of cBFPF is in the expected antiparallel correlation (slope = 1.018) with the DFT chemical shifts of the *cis* isomer (Figure 2b, blue open circles). Remarkably, such a correlation was verified also between the signals attributable to the photoproduct and those calculated for the *trans* isomer (Figure 2b, red open circles).

The analysis of H−C spin−spin coupling effect provided the final confirmation to our structural identification. Indeed, it is widely reported that the vicinal coupling $^3J_{C,H}$ in the ^{13}C−C═C−H motif is stereospecific, as $^3J_{C,H}{}^{trans} > {}^3J_{C,H}{}^{cis}$.[31] Such a difference is strongly pronounced when the carbons are unaffected by γ-effect (such as quaternary carbons).[31] On account of this property, we focused our attention on the quaternary carbonylic C2 (signal at 170.8 ppm in cBFPF) and we determined its vicinal coupling with the vinyl proton HB2 ($^3J_{C2,HB2}$) both in cBFPF and its photoproduct (Figure 2c). To avoid interference from other protons at same bonding distance we collected the ^{13}C NMR spectra by selectively decoupling the methyl protons HA3. Our data showed that native cBFPF is characterized by $^3J_{C2,HB2} = 4.40$ Hz while the photoconverted mixture has $^3J_{C2,HB2} = 8.80$ Hz (Figure 2c). In their pioneering work on azlactone stereoisomerism, Prokof'ev et al. found $^3J_{C2,HB2}{}^{cis} = 5.5$ Hz and $^3J_{C2,HB2}{}^{trans} = 12.5$ Hz for the azlactone precursor of cBFPF.[31] Taking into account both the stereospecific dependence of $^3J_{C,H}$ in the ^{13}C−C═C−H structural motif and the close structural homology between the chromophore and its parent azlactone, these data provided an unequivocal identification of the native and photoconverted forms with cBFPF and tBFPF.

Absorption Spectra of Trans Chromophores and Photoisomerization Quantum Yields. Irradiated chromophore solutions in dioxane-d_6 that had been previously analyzed by ^{1}H NMR were used to prepare solutions of known *cis*−*trans* composition in all the other solvents. From the absorption spectra of these solutions and those of the pure *cis* forms we were able to determine the absorption spectral details for pure *trans* isomers in each solvent (Figure 3a−c, blue traces, and Figures S1−S3 in the Supporting Information). Remarkably, the low-energy band of the *trans* chromophores was red-shifted of 5−15 nm compared to that of the *cis* chromophores, depending on the molecular structure and the solvent nature. Conversely, the high-energy band increased in intensity upon isomerization. These effects seem explainable on account of oscillator-strength transfer to the excitation involving the molecular orbital localized on the phenolic ring (HOMO-3), possibly due to decreased conjugation over the entire chromophore in the *trans* configuration.

The theoretical description of photoisomerization (Supporting Information) shows the direct relationship between the spectral change upon irradiation, the optical characteristics of the pure

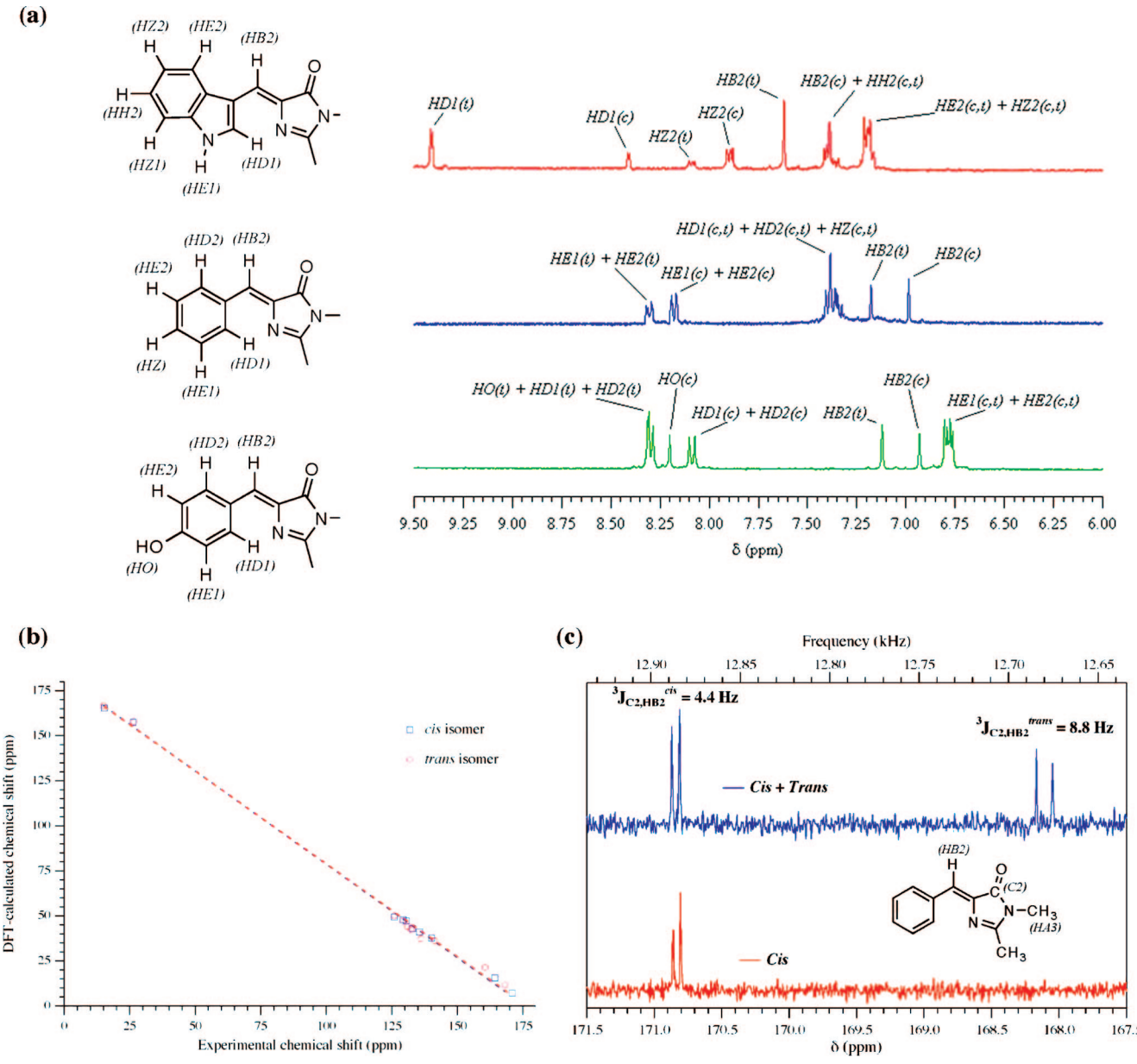

Figure 2. (a) ^{1}H NMR spectra (aromatic region only) of photoconverted cGFP (green line), cBFPF (blue line), and cCFP (red line); molecular structures and peak attribution according to PDB nomenclature is included; resonances of the *cis* and *trans* chromophores are denoted by (c) and (t), respectively. (b) Comparison between DFT-calculated and experimentally measured ^{13}C NMR chemical shifts for cBFPF and tBFPF: excellent correlation was found for all resonances. (c) ^{13}C NMR spectra of native and photoconverted cBFPF while adopting selective decoupling between the methyl protons HA3 and C2: the detected $^{3}J_{C2,HB2}$ values in the photoproduct correspond to those expected for the *cis* and *trans* isomers.

isomers, and the photoisomerization quantum yields. The latter quantities, denoted here as Φ_c(*cis* → *trans*) and Φ_t(*trans* → *cis*), represent the most relevant parameters of the photochromic behavior, as they measure the efficiency of the nonradiative decay channel(s) that lead to the stereochemical change upon light absorption. For moderate optical densities eq S6 (Supporting Information) shows that the solution absorbance follows a first order kinetics upon irradiation, whose amplitude and time-constant are connected to the light power, the solution volume, the extinction coefficients of the two isomers, the thermal recovery rate-constant, and (Φ_c, Φ_t). Accordingly, we fitted the time decays of the low-energy band during the irradiation experiments carried out in methanol to eq S6 (Figure 1b), and, given the knowledge of the other parameters, we calculated the photoisomerization quantum yields for each chromophore in neutral form (Table 1). According to the determined Φ values, the photoisomerization processes are very effective. Remarkably about 100% of the absorbed photons by the *trans* isomers lead to the stereochemical change in the BFPF and CFP chromophores. Note that photoisomerization quantum yields of reported photochromic proteins (GFP chromophore) range between 10^{-6} and 10^{-3}.[10,14]

The Φ_c values were also determined by nanosecond laser flash photolysis experiments. Here, the chromophores were exposed to a single shot of a pulsed 355 nm laser light while monitoring the absorbance changes at 420 nm (cGFP, Figure 1d). Different detection wavelengths were used for cCFP (455 nm) and for cBFPF (390 nm). All chromophores showed an irreversible (on the time scale of the experiment) change in absorbance (ΔA) taking place below the time resolution of the apparatus (5 ns). ΔA was found to increase linearly with laser pulse energy at low values and saturates above ≈ 20 mJ per pulse, as expected

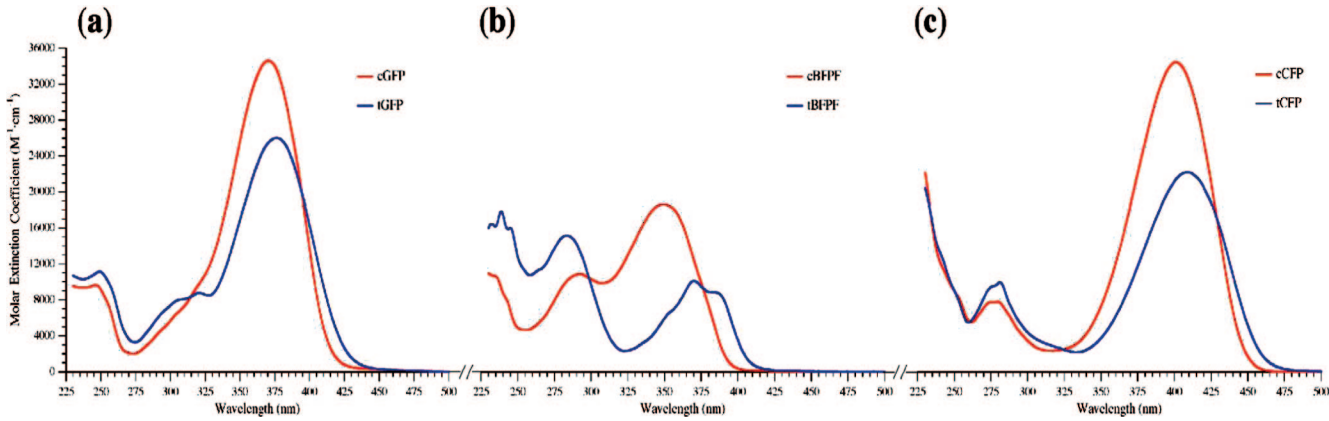

Figure 3. Molar absorption spectra of neutral GFP (a), BFPF (b), and CFP (c) chromophores in methanol. The *cis* and *trans* isomers are reported in red and blue, respectively. The extinction coefficient scale is common for all chromophores in order to allow a comparison of molar absorption values.

for a reversible photoconversion (not shown). Methylene blue was used as an actinometer (Supporting Information) and allowed for the calculation of $\Phi_c$values at different laser powers by means of the comparative method (Supporting Information).[32] Extrapolation to zero laser pulse energy (inset to Figure 1d) yielded the actual Φ_c values (Table 1). Noticeably we found Φ_c values in excellent agreement with those obtained by the continuous irradiation experiment. Furthermore, the obtained Φ_c for cGFP are in good agreement with the value recently reported by Yang et al. for the same chromophore.[29]

Discussion

In recent years, new scientific evidence pointed out that the photophysics of some GFP mutants is not merely restricted to fluorescence emission but comprises other remarkable properties such as photoactivation and reversible photoswitching. The essential role of the detailed folded structure of the protein in determining such phenomena is generally acknowledged. Indeed, the presence of the β-barrel fold in GFP is necessary for fluorescence, since it provides the structural rigidity and the inaccessibility to external quenchers that are prerequisites for the chromophore to emit. The complex photophysics of GFP mutants, however, is ultimately linked to the peculiarities of the chromophore that emerge also when the latter is buried within the tridimensional fold. Notably, the (*Z*)−(*E*) diastereomerization of the chromophore, which is commonly referred to as *cis*−*trans* isomerization, was proposed to be at the basis of fluorescence photoswitching for some GFP mutants[10] and was later demonstrated as an effective mechanism of fluorescence modulation in FPs from *Anemonia* Sulcata[11] and *Clavularia*.[12] From these studies, however, it is still unclear whether the photoinduced *cis*−*trans* isomerization represents a general feature of FP chromophores. The scope of this work was to verify the validity of this hypothesis for three synthetic analogues of GFP chromophores, namely wild type Y66 (GFP), Y66F (BFPF), and Y66W (CFP).

Our investigation started by carrying out DFT-B3LYP theoretical calculations to evaluate the thermodynamic stability of these molecules as function of the stereochemical configurations (defined by the φ and τ dihedral angles, Scheme 1). In this analysis we considered only the neutral state of the ionizable GFP chromophore, in order to allow for a reliable comparison with the other two derivatives. Both in gas phase and in polar media we found that the symmetric phenol/phenyl ring of the GFP or BFPF chromophores leads to just two ground-state configurations, i.e. *cis* ($\tau \approx 0°$) and *trans* ($\tau \approx 180°$), the latter being about 2.5−3.0 kcal/mol less stable than the former (Table 1). This result was confirmed by our experiments: no trace of *trans* isomers was found in the ^{1}H NMR spectra of native cGFP and cBFPF. Differently, calculations on the asymmetric indolyl ring in the CFP chromophore yielded four ground-state configurations, two *cis* (c1CFP, c2CFP) and two *trans* (t1CFP, t2CFP) (Scheme 2). Notably, steric hindrance between the indolyl and the imidazolinone ring leads to a strongly decreased stability of the two $\varphi \approx 180°$ configurations (c2CFP, t2CFP, see Table 1). As a result, t1CFP becomes more stable than c2CFP, and this suggests its being detectably populated at room temperature. The presence of significant *trans* population at room temperature was indeed confirmed by our ^{1}H NMR measurements in methanol. It is worth noting that the calculated free-energy minima were found to correspond to nearly all-planar geometrical arrangements of the chromophores, owing to the formation of an extended electronic conjugation along the two aromatic rings.

Following the identification of the ground states, we demonstrated that all chromophores were reversibly photoconvertible between the *cis* and *trans* forms, regardless of the solvent characteristics (Scheme 1, **iii**−**iv**). In our experiments, we always made use of continuous wave light sources and moderate illumination intensities to avoid triggering of multiphoton processes. Indeed, it has been demonstrated that high photon fluxes, such as those typical of fs- and ps-pulsed excitation, may lead to unexpected photophysics. For example, some authors found that the two-photon photobleaching of GFP is often accompanied by higher-order effects, possibly owing to coherent or sequential higher-order excitation of upper electronic states.[33,34] Note that the *cis*−*trans* photoconversion of the Dronpa chromophore (similar to cGFP/tGFP) has been reported to be a single-photon process at illumination intensities similar to those adopted by us.[35]

Cis−*trans* isomerization was found to be associated with an intensity decrease and red-shift of the low-energy band in the absorption spectrum (Figure 1a and 3). The red-shift of the *trans* spectrum from the *cis* counterpart is not very large (5−10 nm), but allowed us to address selectively each form and to show the reversible photochromism of the chromophores. The structural identification of the native molecules and their photoproducts with the *cis* and *trans* isomers was made possible by ^{1}H NMR/^{13}C NMR analysis (Figure 2). To date only the ^{1}H NMR spectral details of cGFP and tGFP were reported.[27] For cBFPF and tBFPF, ^{13}C NMR data were compared with theoretical calculations and a remarkable agreement between the two data

sets was found (Figure 2b). Furthermore, selectively decoupled ^{13}C NMR spectra allowed for the configurational assignment to cBFPF and its photoproduct on a pure experimental basis (Figure 2c). cBFPF and tBFPF were selected for this analysis on account of their simpler molecular structures and thermal stability in both forms (see below). Notably, ^{1}H NMR allowed the determination the molar fractions of the *cis* and *trans* isomers in the photoconverted mixtures. From these data and the measured optical properties of the mixtures, we were able to reconstruct the molar absorption spectra of pure *trans* chromophores in solvents with different characteristics (Figure 3). To our knowledge, this is the first time that the optical spectra of pure *trans* FP chromophore forms are presented to the scientific community.

tGFP and tCFP were shown not to be stable at room temperature and in protic solvents. They spontaneously reconverted back into their *cis* counterparts (Scheme 1, part **iv**; Figure 1c), consistently with the higher free-energy of the *trans* forms. The decays of tGFP and tCFP were found to be nonmonoexponential, suggesting the presence of reaction intermediates. In aprotic solvents, however, tGFP and tCFP displayed considerable thermal stability. Remarkably, tBFPF was found to be stable for weeks at room temperature in any solvent. It is tempting to attribute this complex phenomenology to proton displacement/rearrangement mechanisms, which may lower the energy barrier between the *trans* and *cis* forms and would be accessible only in protic solvents. The overall kinetic scheme, however, is not quite clear yet. The fast equilibrium between the anionic and neutral GFP chromophore, for which different *cis*−*trans* energy barriers were calculated,[16] cannot explain the presence of slow-forming/slow-degrading intermediates on the route to the stable *cis* isomer. Indeed, although the decay of tGFP was accelerated in water compared to methanol, the recovery rate was rather similar at neutral and alkaline pH.

The kinetic analysis of the photo/thermal isomerization process predicts that, for moderate optical densities (<0.1) and front-face illumination geometry, the chromophore absorbance must follow a monoexponential law (eq S6, Supporting Information). Accordingly, we fitted the experimental photoconversion curves of neutral chromophores to eq S6 (Figure 1b) and, from the knowledge of the irradiation power, the solution volume, and the extinction coefficients of the pure isomers, we determined the photoisomerization quantum yields Φ_c and Φ_t. Φ_c values were also obtained by a flash-photolysis method relying on single-shot irradiation of the chromophores at 355 nm and measurement of the absorption changes extrapolated at zero power. Methanol was selected as solvent for these experiments owing to its mixed protic/organic properties, in an effort to mimic the chromophore environment in the protein. In all cases we found that Φ_c and Φ_t are greater than 0.1, suggesting that photoisomerization gives a major contribution to the deactivation of the excited states of the chromophores. The quantum yield for the photoconversion of cGFP to tGFP is consistent with the value recently determined for the same chromophore system in methanol.[29] Noticeably, tBFPF and tCFP showed Φ_t values close to unity. This indicates that in these chromophores the *trans* excited-state energy surface determines de-excitation pathways almost completely leading to the *cis* configuration. For comparison, the photoisomerization quantum yield of the known photochromic proteins undergoing chromophore *cis*−*trans* isomerization is in the $10^{-6}-10^{-3}$ range.[10,14] This shows that the inclusion within the β-barrel and the establishment of the H-bonding network with the closest protein environment can decrease by several orders of magnitude the efficiency of chromophore photoisomerization. Such a difference highlights how the stereochemical freedom of the protein chromophore determines the accessibility of the photoisomerization channel. Significantly, many authors have attributed the determining factor of FP photochromism to a loss of structural rigidity around the chromophore.[12,14,15] It is also likely that other typical processes in FPs, such as proton transfer reactions, are powerful modulators of the stereoisomerization, eventually affecting the overall efficiency of photoconversion.[36,37] It is worth noting the inhibiting effect of proton donor moieties on the photoisomerization mechanism has been recently pointed out for some model chromophores in protic solvents.[29]

In conclusion, we demonstrated that the *cis*−*trans* isomerization is a common deactivation channel of the excited-state of FP model chromophores. By means of a thorough NMR analysis combined with DFT calculations, we were able to attribute the stereochemistry of initial compounds and their photoproducts. For the first time we reported the optical absorption spectra of neutral *trans* chromophore analogues and the values of photoisomerization quantum yields. The comparison with the data available for the reported photochromic proteins suggests that the chromophore environment plays a decisive role in determining the effectiveness of the photoinduced *cis*−*trans* isomerization.

Interestingly, the *trans* states of ionizable chromophores are unstable in protic solvents and decay back to the correspondent *cis* states in times ranging from few minutes to hours. This result is consistent with the much higher thermodynamical stability calculated for the *cis* isomers by our DFT analysis. Nonetheless, our DFT analysis indicates that the CFP chromophore should be characterized by a rather stable *trans* conformation, owing to the steric hindrance of the indolyl lateral group. The presence of detectable *trans* CFP chromophore at room temperature was experimentally verified by ^{1}H NMR measurements. The characteristics of the thermal relaxation phenomenon indicate that mobile protons/hydrogen bonds play a relevant role in determining the activation energy barrier between the *trans* and *cis* states.

Acknowledgment. We thank Dr. Valentina Tozzini, Dr. Stefano Luin and Dr. Guido Pintacuda for stimulating discussions. Partial financial support by MUR within FIRB Project RBLA03ER38 is gratefully acknowledged.

Supporting Information Available: Text giving details of the procedure synthesis of the chromophores, the theoretical description of the isomerization's kinetics, and the description of experimental setup for laser flash-photolysis and figures showing the molar absorption spectra of pure *cis*−*trans* isomers in all tested solvents. This material is available free of charge via the Internet at http://pubs.acs.org.

References and Notes

(1) Tsien, R. Y. *Annu. Rev. Biochem.* **1998**, *67*, 509.
(2) Miyawaki, A. *Neuron* **2005**, *48*, 189.
(3) Wachter, R. M. *Acc. Chem. Res.* **2007**, *40*, 120.
(4) Tozzini, V.; Pellegrini, V.; Beltram, F. Green Fluorescent Proteins and their applications to cell biology and bioelectronics. In *CRC Handbook of Organic Photochemistry and Photobiology*; Horspool, W., Lenci, F., Eds.; CRC Press: Boca Raton, FL, 2004; p 139.
(5) Heim, R.; Prasher, D. C.; Tsien, R. Y. *Proc. Natl. Acad. Sci. U.S.A.* **1994**, *91*, 12501.
(6) Ting, A. Y.; Kain, K. H.; Klemke, R. L.; Tsien, R. Y. *Proc. Natl. Acad. Sci. U.S.A.* **2001**, *98*, 15003.
(7) Patterson, G. H.; Lippincott-Schwartz, J. *Science* **2002**, *297*, 1873.
(8) Gurskaya, N. G.; Verkhusha, V. V.; Shcheglov, A. S.; Staroverov, D. B.; Chepurnykh, T. V.; Fradkov, A. F.; Lukyanov, S.; Lukyanov, K. A. *Nat. Biotechnol.* **2006**, *24*, 461.

(9) Cinelli, R. A. G.; Pellegrini, V.; Ferrari, A.; Faraci, P.; Nifosi, R.; Tyagi, M.; Giacca, M.; Beltram, F. *Appl. Phys. Lett.* **2001**, *79*, 3353.
(10) Nifosi, R.; Ferrari, A.; Arcangeli, C.; Tozzini, V.; Pellegrini, V.; Beltram, F. *J. Phys. Chem. B* **2003**, *107*, 1679.
(11) Andresen, M.; Wahl, M. C.; Stiel, A. C.; Grater, F.; Schafer, L. V.; Trowitzsch, S.; Weber, G.; Eggeling, C.; Grubmuller, H.; Hell, S. W.; Jakobs, S. *Proc. Natl. Acad. Sci. U.S.A.* **2005**, *102*, 13070.
(12) Henderson, J. N.; Ai, H. W.; Campbell, R. E.; Remington, S. J. *Proc. Natl. Acad. Sci. U.S.A.* **2007**, *104*, 6672.
(13) Andresen, M.; Stiel, A. C.; Trowitzsch, S.; Weber, G.; Eggeling, C.; Wahl, M. C.; Hell, S. W.; Jakobs, S. *Proc. Natl. Acad. Sci. U.S.A.* **2007**, *104*, 13005.
(14) Habuchi, S.; Ando, R.; Dedecker, P.; Verheijen, W.; Mizuno, H.; Miyawaki, A.; Hofkens, J. *Proc. Natl. Acad. Sci. U.S.A.* **2005**, *102*, 9511.
(15) Loos, D. C.; Habuchi, S.; Flors, C.; Hotta, J.; Wiedenmann, J.; Nienhaus, G. U.; Hofkens, J. *J. Am. Chem. Soc.* **2006**, *128*, 6270.
(16) Weber, W.; Helms, V.; McCammon, J. A.; Langhoff, P. W. *Proc. Natl. Acad. Sci. U.S.A.* **1999**, *96*, 6177.
(17) Nifosì, R.; Amat, P.; Tozzini, V. *J. Comput. Chem.* **2007**, *28*, 2366.
(18) Kojima, S.; Ohkawa, H.; Hirano, T.; Maki, S.; Niwa, H.; Ohashi, M.; Inouye, S.; Tsuji, F. *Tetrahedron Lett.* **1998**, *39*, 5239.
(19) Banderini, A.; Sottini, S.; Viappiani, C. *Rev. Sci. Instrum.* **2004**, *75*, 2257.
(20) VanBrederode, M. E.; Gensch, T.; Hoff, W. D.; Hellingwerf, K. J.; Braslavsky, S. E. *Biophys. J.* **1995**, *68*, 1101.
(21) Cossi, M.; Barone, V. *J. Chem. Phys.* **2001**, *115*, 4708.
(22) Ruud, K.; Helgaker, T.; Bak, K. L.; Jørgensen, P.; Jensen, H. J. A. *J. Chem. Phys.* **1993**, *99*, 3847.
(23) Frisch, M. et al. Gaussian Inc.: Pittsburgh, PA; revision B.03 ed., 2003.
(24) Mukerjee, A.; Kumar, P. *Heterocycles* **1981**, *16*, 1995.
(25) Rao, Y.; Filler, R. *Synthesis* **1975**, *12*, 749.
(26) Berman, H.; Westbrook, J.; Feng, Z.; Gilliland, G.; Bhat, T.; Weissig, H.; Shindyalov, I.; Bourne, P. *Nucl. Acids. Res* **2000**, *28*, 235.
(27) He, X.; Bell, A. F.; Tonge, P. J. *FEBS Lett.* **2003**, *549*, 35.
(28) Bell, A. F.; He, X.; Wachter, R. M.; Tonge, P. J. *Biochemistry* **2001**, *40*, 8619.
(29) Yang, J.; Huang, S.; Liu, Y.; Peng, S. *Chem. Commun.* **2008**, 1344.
(30) Morgenstern, A.; Schutij, C.; Nauta, W. *Chem. Commun.* **1969**, 321.
(31) Prokof'ev, E.; Karpeiskaya, E. *Tetrahedron Lett.* **1979**, *8*, 737.
(32) Bensasson, R. V.; Land, E. J.; Truscott, T. G. *Excited states and free radicals in biology and medicine*; Oxford University Press: Oxford, U.K., 1993.
(33) Mondal, P. P.; Diaspro, A. *Phys. Rev. E: Stat. Nonlin. Soft Matter Phys.* **2007**, *75*, 061904.
(34) Patterson, G. H.; Piston, D. W. *Biophys. J.* **2000**, *78*, 2159.
(35) Habuchi, S.; Dedecker, P.; Hotta, J.; Flors, C.; Ando, R.; Mizuno, H.; Miyawaki, A.; Hofkens, J. *Photochem. Photobiol. Sci.* **2006**, *5*, 567.
(36) Schafer, L. V.; Groenhof, G.; Boggio-Pasqua, M.; Robb, M. A.; Grubmuller, H. *PLoS Comput. Biol.* **2008**, *4*, e1000034.
(37) Fron, E.; Flors, C.; Schweitzer, G.; Habuchi, S.; Mizuno, H.; Ando, R.; Schryver, F. C.; Miyawaki, A.; Hofkens, J. *J. Am. Chem. Soc.* **2007**, *129*, 4870.

JP802419H